Nigerian Research Journal of Chemical Sciences **(ISSN: 2682-6054)**
Vol. 7, 2019

SYNTHESIS AND CHARACTERIZATION OF ZINC FERRITE AND ZINC/SILICA GEL COMPOSITE PHOTOCATALYSTS

*IBRAHIM, D., PAUL, E. D., YASHIM, Z. I.

Department of Chemistry, Ahmadu Bello University, Zaria, Nigeria

*Corresponding Author: thrbrhm@gmail.com

ABSTRACT

Zinc Ferrite, $ZnFe_2O_4$, and Zinc Ferrite/silica gel composite, $ZnFe_2O_4/SiO_4$, in varying proportions (10 wt%, 20 wt%, 30 wt% and 40 wt%) were synthesized via co-precipitation method and characterized using X-ray Diffraction, XRD, and Scanning Electron Microscope, SEM. The average particle size and specific surface area were determined. The X-ray Diffraction, scanning electron microscope, average particle size and surface area revealed that the crystalinity of the material increased with increase in the loading of the SiO_2 as support, with average particle size increasing from 10 wt% $ZnFe_2O_4/SiO_4$, 20.1 nm and 40 wt% $ZnFe_2O_4/SiO_4$, 72.4 nm. However, the specific surface area decreased from 390 nm to negative results.

Keywords: Average particle size, silica gel, surface area, XRD, zinc ferrite

INTRODUCTION

Zinc ferrites are a series of synthetic inorganic compounds of zinc and iron (ferrite) with the general formula of $Zn_xFe_{3-x}O_4$. Zinc ferrite compounds can be prepared by aging solutions of $Zn(NO_3)_2$, $Fe(NO_3)_3$, and triethanolamine in the presence and in the absence of hydrazine [1].

At the present, one of the most interesting and challenging issues of the science of magnetic nanoparticles is the introduction of new electronic, optical or photochemical properties and optimization of their magnetic properties. Zinc ferrite has attracted more attentions due to its interesting magnetic property [2].

Zinc ferrite nanoparticles are under intense research because of their unique chemical, mechanical and structural properties [3]. Ferrite nanoparticles have versatile application in catalysis, electronics, photonics, sensors and fero fluids [4]. Many types of methods including ceramic synthesis [5], co-precipitation method [6, 7], tartrate precursor method [8], have been used to fabricate the precursor. Co-precipitation method has been intensively investigated to

synthesize the precursor. For example, zinc ferrite could be synthesized at 650°C for 6 hours which greatly reduces the production cost [8].

In view of the facts about the application of zinc ferrite especially in the photocatalysis, therefore a need to synthesize and characterize the zinc ferrite so also to be optimized by using support with other semi-conductor such as silica gel.

In this research work, zinc ferrite and zinc ferrite silica get composite photocatalysts were synthesized, characterized and then its photocatalytic activity evaluated by degradation of methylene blue.

MATERIALS AND METHODS

Synthesis of $ZnFe_2O_4$ and $ZnFe_2O_4$/Silica gel

About 25.5 g zinc chloride and 69 g Iron chloride were made with 300 mL distilled water separately. It was then mixed in a 2000ml conical flask with vigorous stirring at 70°C and 70 g. 300 mL of dilute sodium hydroxide was then added slowly at constant rate of adding and stirring to the mixed solution of zinc chloride and iron chloride. The precipitate formed (Eq.1) was aged for 24 hours, then filtered and washed thoroughly for several times with distilled water to remove any trace of sodium hydroxide. To further remove water, the solid was vacuum filtered using vacuum filtration pump. The solid was then calcined at 500°C for 3hrs, to yield $ZnFe_2O_4$ (Eq.2)

$$ZnCl_2 + 2FeCl_3 + 8NaOH \longrightarrow Zn(OH)_2 + 2Fe(OH)_3 + 8NaCl \quad (1)$$

$$Zn(OH)_2 + 2Fe(OH)_3 \xrightarrow{500^oC \text{ for } 3hrs} ZnFe_2O_4 + 4H_2O \quad (2)$$

$ZnFe_2O_4$ and Silica gel in various proportion (10 wt%, 20 wt%, 30 wt% and 40 wt%) was then finally dispersed in aqueous suspension with vigorous stirring at a temperature of 50°C for 1hour to yield $ZnFe_2O_4/SiO_2$.

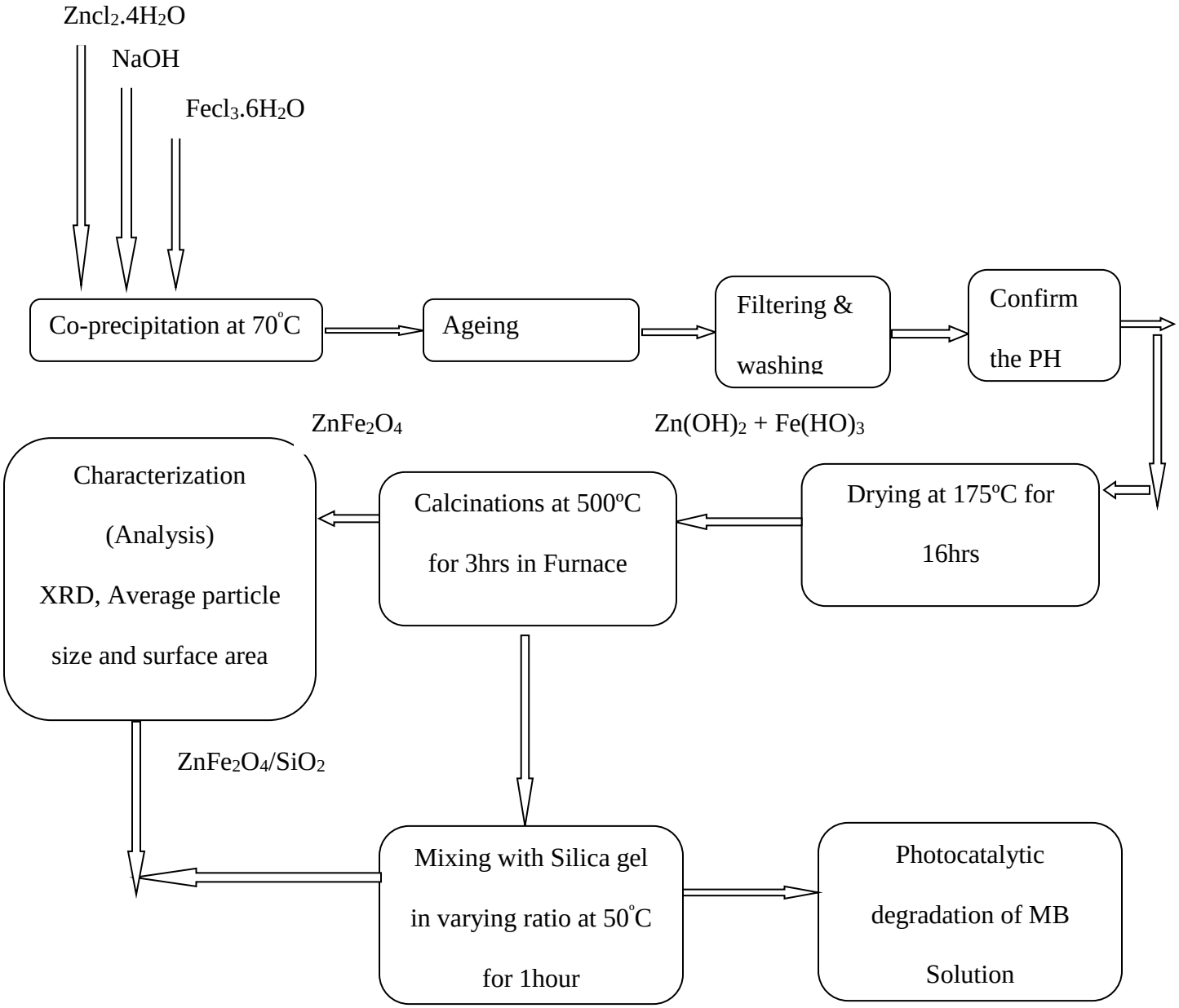

Fig. 1: Block diagram to obtained zinc ferrite and zinc ferrite silica gel composites photocatalysts

Characterization of the Synthesized $ZnFe_2O_4$ photocatalysts and $ZnFe_2O_4/SiO_2$ Composite Photocatalysts

X-Ray diffraction spectroscopy

Empyrel X-Ray diffraction machine was used to examine the crystal structures of the synthesized photocatalysts particles. It is a method of determining the arrangement of atoms within a crystal, in which a beam X-ray strikes a crystal and diffracts into many specific directions using a diffractometer. It provides detailed information on the crystallographic structure and physical properties of materials and thin films.

SEM Analysis

A scanning electron microscope is a type of electron microscope that produces image of a sample by scanning it with a focused beam of electron. The electrons interact with atoms in the sample, producing various signals that contained information about the sample surface topography and composition. The electron beam is generally scanned in a raster scan pattern, and the beam's position is combined with detected signal to produce an image [9].

Specific Surface Area Determination

The surface area was estimated using Sear's method by agitating 1.5g of powdered sample in 100ml of diluted hydrochloric acid and 3.30g of sodium chloride was then added with a constant stirring and the volume was made up to 150ml with de-ionized water. The solution was titrated with 0.10N NaOH and the volume was raised from the pH of 4 to 9 and recorded. Then the surface area of synthesized photocatalysts was estimated [10].

Decolouration of Methylene Blue Solution Using Photolysis

A 100 ml/L stock solution of methylene blue was prepared using distilled water for all the experiments. The adsorption tests were carried out under dark condition, for the evaluation of the adsorption-desorption equilibrium of methylene blue on the surfaces of synthesized photocatalysts. 100 ml of solution of the methylene blue was taken from the stock solution, put in a beaker at a room temperature in dark with stirring for three and half hours. After the first hour of stirring, irradiation for two and half hours was provided with 500 W halogen lamp. An aliquot of 5 ml was then withdrawn from the beaker at an interval of 10 minutes for 1 hour. Some physicochemical parameters: biochemical oxygen demand, chemical oxygen demand, electrical conductivity, pH, turbidity and total dissolved solids, were also carried out.

Photocatalytic Degradation of Methylene Blue Solution

100 ml of solution of methylene blue solution was taken from the stock solution, put in a beaker; 0.1 g of photocatalysts ($ZnFe_2O_4$) was added. The suspension was kept in a dark at room temperature with continuous stirring using magnetic stirrer. After an hour in the dark, the suspension was then irradiated with 500 W halogen lamp. An aliquot of 5 ml was taken from the beaker at interval of 10 minutes for 1 hour, the catalysts were filtered and then analysed using UV-Vis Spectrophotometer to evaluate the photocatalytic degradation. Same procedure was repeated for $ZnFe_2O_4/SiO_2$ variations (10 wt%, 20 wt%, 30 wt% and 40 wt%). Some physicochemical parameters: biochemical oxygen demand, chemical oxygen demand, electrical conductivity, pH, turbidity and total dissolved solids were also carried out.

RESULTS AND DISCUSSION

X-RAY DIFFRACTION PATTERN OF PREPARED ZINC FERRITE AND ZINC FERRITE SILICA GEL

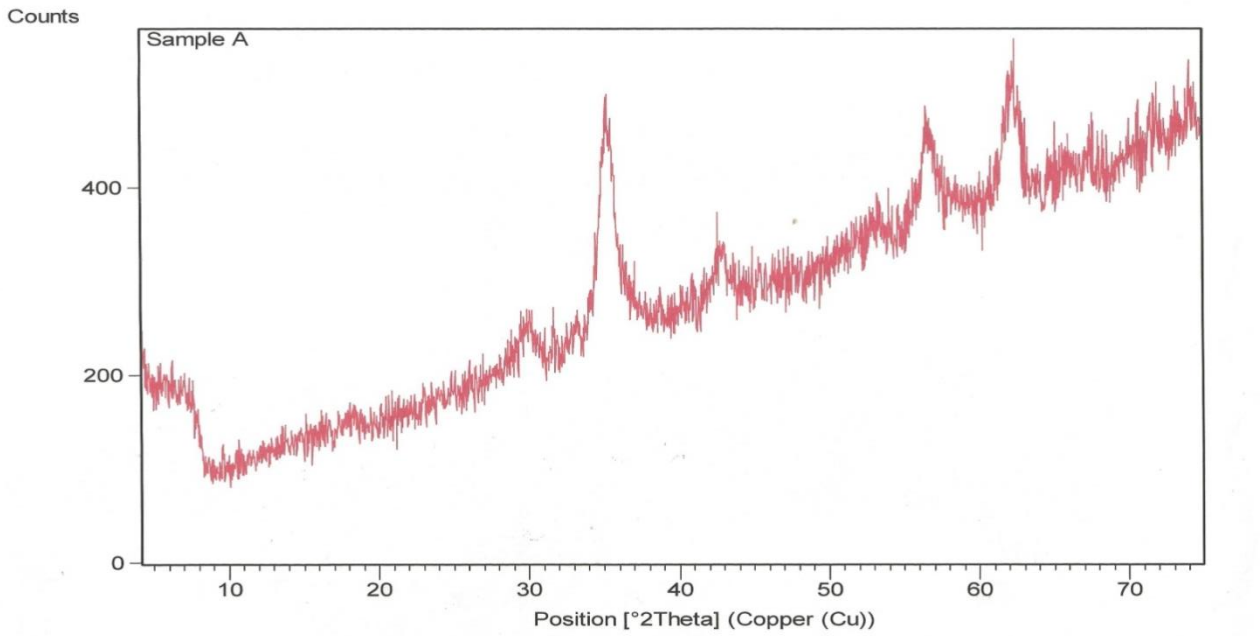

Fig. 2: XRD patterns of the prepared $ZnFe_2O_4$

The figure above shows the X-Ray Diffraction pattern of the prepared pure zinc ferrite without the composite which was characterized by broad low peak

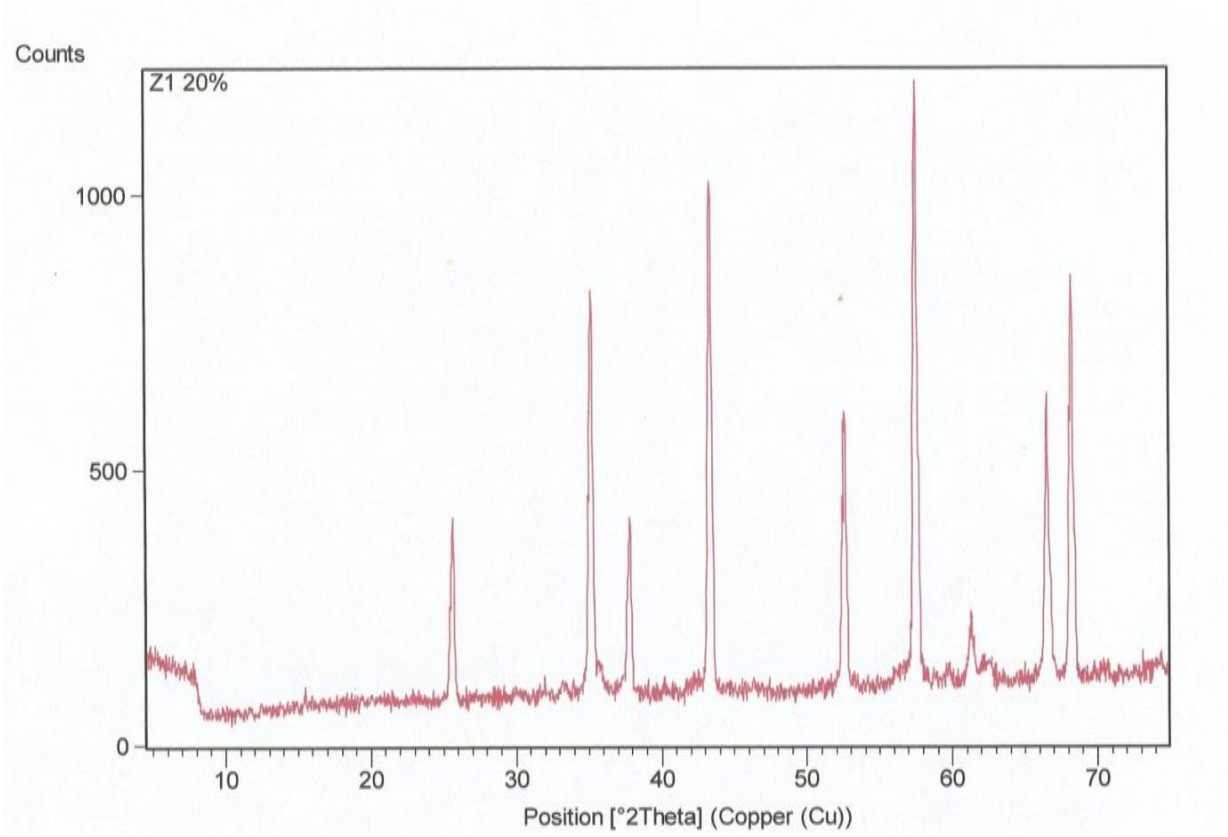

Fig. 4: XRD pattern of the prepared 20 wt% $ZnFe_2O_4/SiO_2$

The figure above shows the X-Ray Diffraction pattern of the prepared zinc ferrite on 20 wt% silica gel support which features sharp peaks and increase in the sharpness of the peaks.

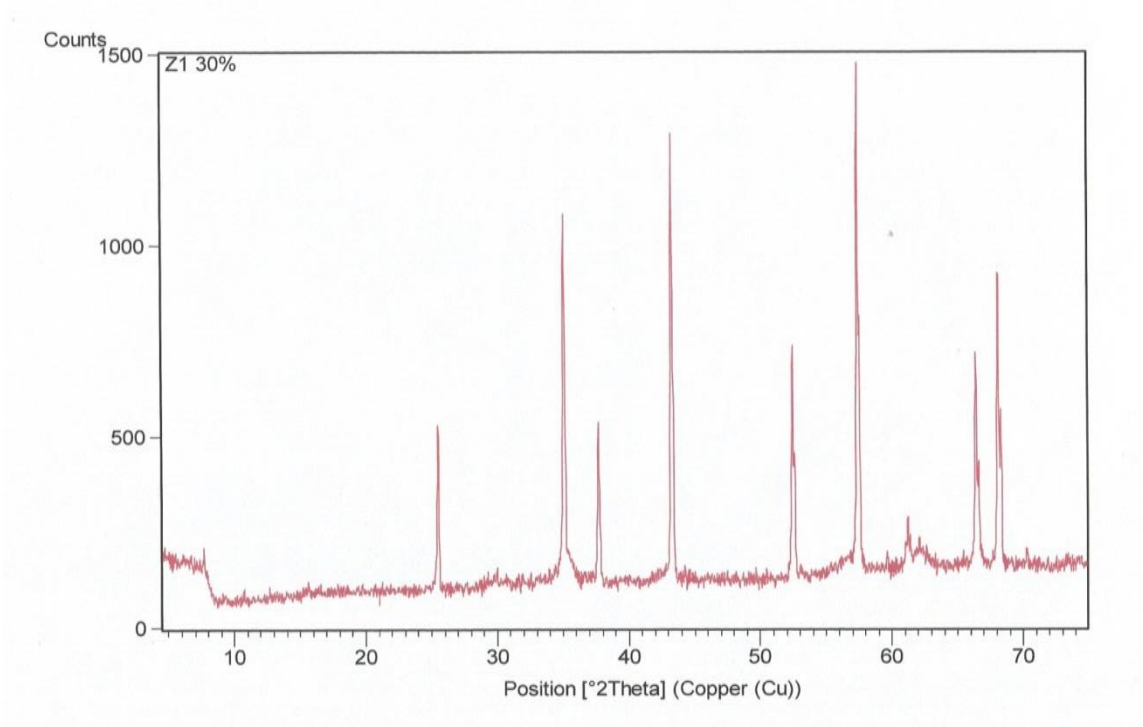

Fig 5: XRD pattern of the prepared 30 wt% $ZnFe_2O_4/SiO_2$

The figure above shows the X-Ray Diffraction pattern of the prepared zinc ferrite on 30 wt% silica gel composites. This also features sharp peaks in which there is an increase in the sharpness of the peaks

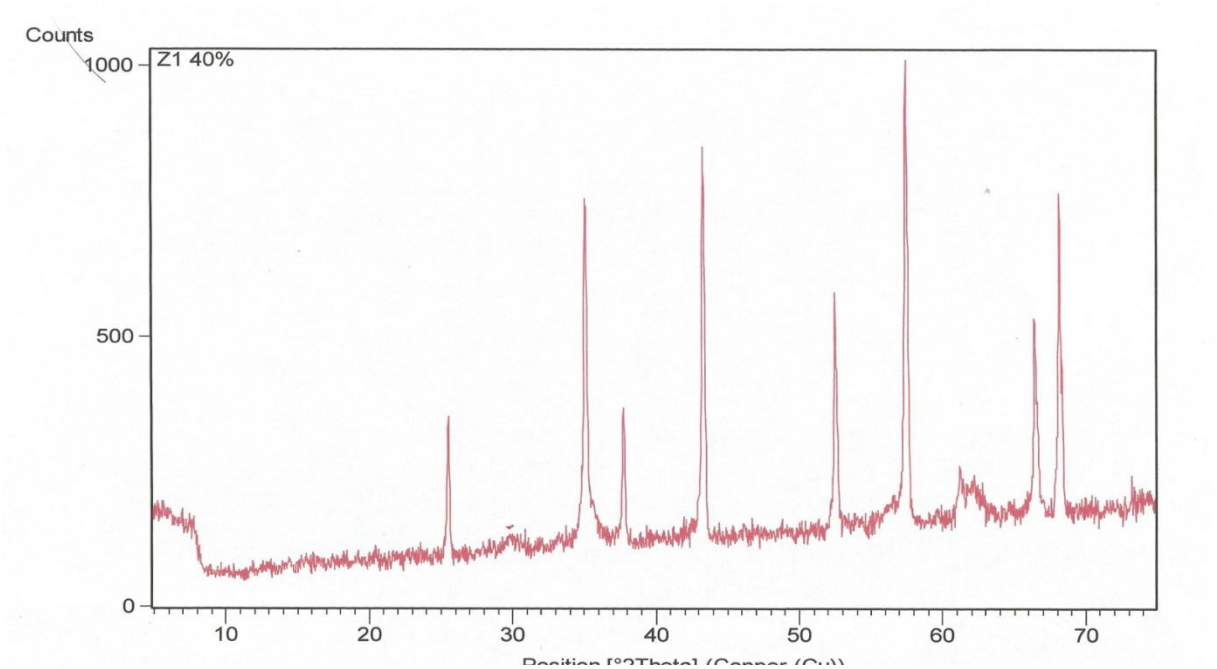

Fig.6: XRD pattern of the prepared 40 wt% $ZnFe_2O_4/SiO_2$

The figure above shows X-Ray Diffraction pattern of the prepared zinc ferrite on a support of 40 wt% silica gel support which also features sharp peaks and evidence of the unperturbed nature of

Table 2: Average particle sizes and specific surface areas of the synthesized $ZnFe_2O_4$ and SiO_2 supported $ZnFe_2O_4$

Photocatalysts	Average particle size (mm)	Specific Surface Area (m^2/g)
$ZnFe_2O_4$	17.2	390
10 wt% $ZnFe_2O_4/SiO_2$	20.1	255
20 wt% $ZnFe_2O_4/SiO_2$	32.0	180
30 wt% $ZnFe_2O_4/SiO_2$	57.3	79
40 wt% $ZnFe_2O_4/SiO_2$	75.4	NA

Note: the negative volume was obtained due to the small volume of the material at the 40 wt%

Table above shows the average particle size, specific surface area of the prepared zinc ferrite, zinc ferrite with the loading (composites) of 10, 20, 30 and 40 wt% photocatalysts.

Morphology of the synthesized zinc ferrite and zinc ferrite silica gel composite

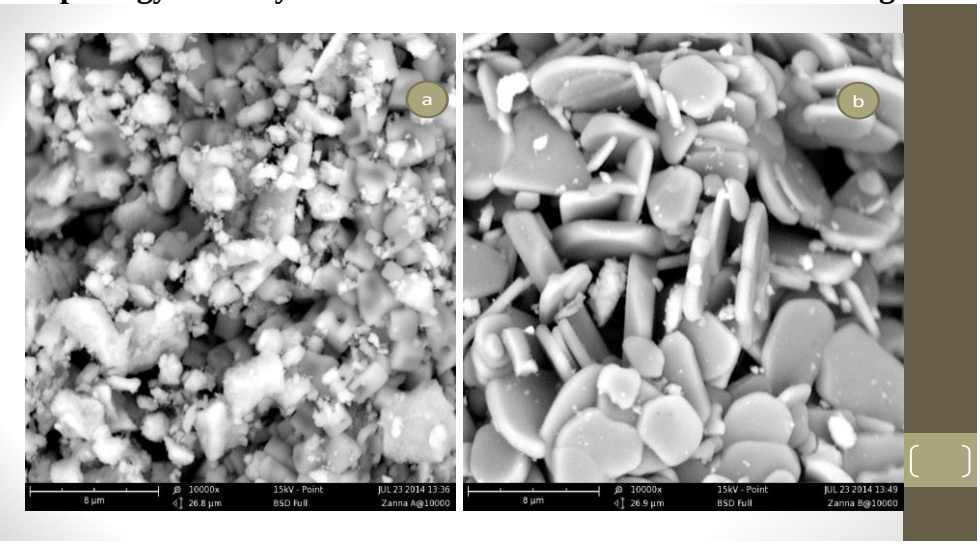

Fig 7: SEM image of (a) pure $ZnFe_2O_4$ and (b) $ZnFe_2O_4/SiO_2$ composite

The figure above shows the SEM image of the prepared pure zinc ferrite in Figure 7a and the 30 wt% zinc ferrite silica gel composite photocatalyst in Figure 7b.

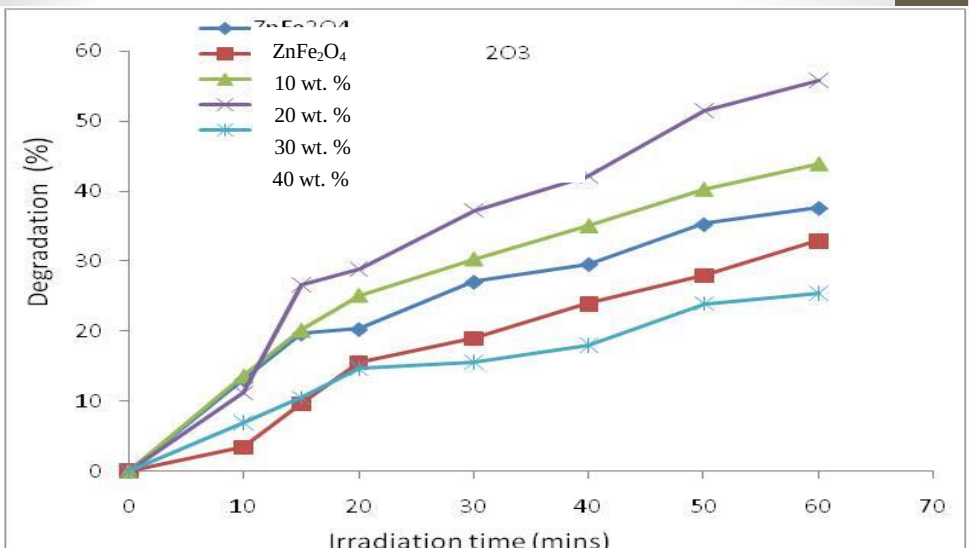

Fig.8: Photocatalytic degradation of MB using $ZnFe_2O_4$ and SiO_2 Supported $ZnFe_2O_4$

The figure above shows the photocatalytic evaluation of the prepared zinc ferrite, 10 wt% zinc ferrite silica gel, 20 wt% zinc ferrite silica gel, 30 wt% zinc ferrite silica gel and 40 wt% zinc ferrite silica gel composite on degradation of methyelene blue.

The XRD pattern of the prepared $ZnFe_2O_4$ displayed in Figure 2 was characterized by broad low intense peaks at Bragg angles (JCPDS card No 82 – 1049). The broad peaks were due to the low crystallinity of the prepared $ZnFe_2O_4$ at 500 ºC. The calcination temperature at 500 ºC was selected based on the work of [11] which established that $ZnFe_2O_4$ sintered at 500 ºC exhibits the highest photocatalysts activity. Higher sintering temperature leads to increase in the crystals size of materials thereby decreasing their specific surface area. The XRD pattern of SiO_2 supported $ZnFe_2O_4$ in figure 3features sharp peaks (JCPDF 75 – 1862). The sharpness of the peaks increased in figure 4.The crystal structures of the SiO_2 remains unperturbed after $ZnFe_2O_4$ loading as observed through Figures 2-4. Similar trend was reported in the work of [12]. The average particles sizes of the synthesized $ZnFe_2O_4$ and SiO_2 supported $ZnFe_2O_4$ was calculated using the Debye-Scherrer equation shown below:

$$Γ=\frac{k\lambda}{\beta cos\theta} \qquad (3)$$

Where: Γ is the particle size,

λIs the wavelength of X- ray diffraction (Cu K α = 0.1542 nm),

K is the sharp factor (K= 0.94),

β is the line width at half maximum height and Θ is the angle position of the maximum peak [13].

From Table 1 it could be observed that the average particle size increased with increase in the weight percentage of SiO_2 supported $ZnFe_2O_4$, whereas, the surface area decreased with increase in the average particle size. Similar trend was observed in the work of [14].

The specific surface area of the synthesized $ZnFe_2O_4$ and SiO_2suported $ZnFe_2O_4$was measured using the Sear's method. As observed from the table, the specific surface area of the unsupported $ZnFe_2O_4$ is 397 m^2/g while with loading at 40 wt% is 75.2 m^2. It has been reported that the surface area of the photocatalysts mostly decreases with increase in the molar ratio of the active component on the support material [8].

Figure 7 indicates that 30 wt% $ZnFe_2O_4/SiO_2$ has high average particle size and the lowest pecific surface area. Therefore its morphological characteristic was considered with the bare zinc ferrite. This was also confirmed with the photocatalytic activity of the synthesized photocatalysts on the decolouration of methylene blue shown in Fig 7.

The morphological characteristic of the synthesized $ZnFe_2O_4$ and 30 wt% $ZnFe_2O_4/SiO_2$ were investigated by SEM analysis. The SEM image of $ZnFe_2O_4$ sample displayed in fig. 6a shows that $ZnFe_2O_4$ exhibited a compact arrangement of nanoparticles with roughly irregular shape. Most of the particles are aggregated which make it difficult to determine the exact size and the shape of the particle [15]. The SEM image 30wt% $ZnFe_2O_4/SiO_2$ presented in Fig.6b, reveals that SiO_2 exhibits a plate/disk- like shape and $ZnFe_2O_4$ is deposited on its surface. SiO_2 is more crystalline than $ZnFe_2O_4$.

The photocatalytic activity of the prepared photocatalysts was evaluated using methylene blue dye. Methylene blue is used as test molecule for evaluating the activity of series of photocatalyst. The effect of varying $ZnFe_2O_4$ loading (10, 20, 30 and 40 wt%) on SiO_2 support were investigated at an initial methylene blue concentration of 50mg/l with a photocatalyst dosage of 1.0g/l. It is seen in Figure8 that the percentage photocatalytic degradation of MB increases with increase in the $ZnFe_2O_4$ loading from 10 wt% to 30 wt% due to the increase in the number of $ZnFe_2O_4$ active sites because photocatalytic degredation occurs at the active sites. However, percentage photocatalytic degredation of methylene blue decreased when $ZnFe_2O_4$ loading increased to 40 wt%. The significant reduction of the photocatalytic activity of sample containing 40 wt% $ZnFe_2O_4$ can be attributed to the increased agglomeration of $ZnFe_2O_4$ particle

on SiO_2 thereby decreasing the rate of diffusion of photogenerated electron-hole pairs onto the methylene blue molecules at the interface of solid photocatalyst methylene blue solution. Retardation of the diffusion of electron-pairs decreases the extent of photocatalytic degredation [16]. in the present work, highest photocatalytic degredation of MB was achieved with 30 wt% $ZnFe_2O_4/SiO_2$.

CONCLUSION

Zinc ferrite and zinc ferrite silica gel composite photocatalysts were synthesized via co-precipitation methods and characterized using X-ray Differaction,Scaning Electron Miscroscope, surface area determination and average particle size. The results revealed that the crystalinity of the material increases with the loading of the support from 10 wt% to 40 wt %, while the 30 wt% gave the best photocatalytic activity.

REFERENCES

1. Andrés, V., Martinez, M. & Matijevié, E. (1993). Synthesis and characterization of zinc ferrite particles prepared by hydrothermal decomposition of zinc chelate solutions. *Journal of Materials Research*. 8(11), 2916A.
2. Yao, C., Zeng, Q., Gayo, F., Torres, T., Liu, J., Wu, H., Ge, M. & Jiang, J. (2007). Introduction of new electronic, optical or photochemical properties and optimization of their magnetic properties. *Journal of Physical Chemistry*, 111,12274
3. Darriel, M. L., Bernett, D.S., Lashmore, P., Lubtiz, M., Rubinstein, W. L. & Lechter, M.Z. (1987). Properties of electrodeposited Co-Cu multilayer structures, *Journal of Applied Physics*., 61,4067
4. Hou, X., Feng, J. Xu, X. & Zhang, M. (2000). Synthesis and characterization of spinel $MnFe_2O_4$nanorod by seed-hydrothermal route. *Journal of Alloy compound*, 491, 258-263.
5. Chinnasamy, C. N., Narayanasamy, A. & Ponpandian, N. (2000). Magnetic properties of nanostructural ferromagnetic zinc ferrite. *Journal of Physical Materials.* 12**,** 7795.
6. Makovec, D., Kodre, A., Arcon, I. & Dronfenic, M. (2009). Functionalization of magnetic nano-particles with 3-aminopropyl silane. *Journal of Nanoparticles Resources* .11,1145

7. Makovec, D., Kodre, A., Arcon, I. & Dronfenic, M. (2011). The structure of compositionally constrained zinc-ferrite spinel nano-particle. *Journal of Nanoparticles Resources*. 13**,** 1981
8. Kostedt, I. V., Drwiega, J. W. Mazyck, D.W. Lee, S., Sigmund, W., Wu, C. & Chadik, P. (2010). Magnetically agitated photocatalytic reactor for photocatalytiv oxidation of aqueous phase organic pollutants. Journal *of Environmental Science Technology*, 39, 8052-8056
9. McMullan, D. (2006). Scaning electron microscopy 1928-1965 scaning. **17** (3), 175-185
10. Sears, G.W. (1981). Determination of specific surface area by titration with sodium hydroxide. *Journal of Analytical Chemistry,* 28,33-45
11. Jadhav, S.D., Hankare, P. P., Patil, R.P. & Sasikala, R. (2010). Effect of sintering on Photocatalystic degradation of methyl orange using zinc ferrite. *Journal of material letter*, 65, 371 -373
12. Farbod, M. andKhademalrasool, M. (2011). Synthesis of TiO2 nanoparticles by Vasodilatory shock during cardiopulmonary bypass. Anaesthesia, 60: 575-587
13. Hao, O. J., Kim, H. & Chiang, P.C. (2000). *Decolorization of waste water*. Critical Reviews in Environmental Sciences, **30**,449- 505.
14. An, T. C., An, J. B., Yang, H., Li, G. Y., Feng, H. X. & Nie, H.P.(2011). Photocatalytic degradation, kinetic and mechanism of antivirus drug-lamivudine in TiO_2 Dispersion. *Journal of Hazardous Material*, 197, 229-236
15. Kim, T. Y., Lee, Y., Park, K., Kim, S. J. & Cho, S.Y. (2010). A study of photocatalytic of TiO_2 coated onto chitosan beads and activated carbon. Research on Chemical Interface, 31, 343-358.
16. Li, G.Z., Park, S., Kang, D.W., Krajmalnik-Brown, R. & Ritmann, B.E. (2011). 2, 4, 5-trichlorophenol degradation using a novel TiO_2-Coated biofilm carrier: Roles of adsorption, photocatalysis, and biodegradation. *Journal of Environmental Science Technology*, 45, 8359-8367